

Etch Rate Modeling in MEMS Design ^{*†}

Ted J. Hubbard[†]

Erik K. Antonsson[§]

Engineering Design Research Laboratory
Division of Engineering and Applied Science
California Institute of Technology

January 25, 1995

Abstract

This paper presents an etch rate model for determining the full three dimensional behavior of an etchant from experimentally determined etch rates of four principal planes: (100), (110), (111), & (311). The etch rate for an arbitrary plane is expressed in terms of the measured planes. The model shows excellent agreement with both experimental measurements and values reported in the literature. A high quality 3D model of etch rates, such as the one reported here, is required for MEMS CAD or etch simulators to be able to accurately predict etched shapes.

1 Introduction

Any MEMS CAD system that will accurately be able to determine a mask shape for a given desired three dimensional fabricated shape will require well characterized and accurate three dimensional etch rate information. Similarly three dimensional etch simulators [1, 2, 3, 4], such as the author's Eshape and Cellular Automata methods [5, 6] as well as the Slowness method by Sequin [7] and ASEP by Buser [8] require accurate etch rate data. The rate of etching is dependent on the orientation of the face being etched in the crystal. These differing rates mean that most etched shapes change with time. In order to simulate the time evolution of three dimensional etched shapes, it is essential that the full etch rates in all directions be well known.

Unfortunately, for most etchants etch rates for only a few major planes are known, notably the (100), (110), (111), and perhaps the (311) planes [9, 10, 11, 12,

^{*}Manuscript prepared for submission to the *IEEE/ASME Journal of Microelectromechanical Systems*

[†]Word Count: 2800 words.

[‡]Graduate Research Assistant

[§]Corresponding author: Associate Professor of Mechanical Engineering, Mail Code 104-44, Caltech, Pasadena, CA 91125, FAX: 818/568-2719, e-mail: erik@design.caltech.edu

13]. Seidel [12], for example has studied the etch rate behavior of KOH in both the (100) and (110) planes. The (100) plane etch rate diagram has a characteristic four lobed rosette pattern while the (110) plane etch rate diagram is six-sided. These planes are chosen because they tend to dominate most etched shapes, but they do not give the full picture. In this paper we will derive a model which supplies the full etch rate diagram given a few experimentally measured planes. The model requires a minimum of N planes to provide a N dimensional representation, but more planes may be utilized if they are available, providing a more accurate etch rate diagram. The model will first be derived for two dimensions with two parameters, then with three parameters. The same approach will be used for the three dimensional models with three and four parameters. The models show excellent agreement with both experimental measurements and values reported in the literature.

2 Two Dimensions

We represent etch rates with vectors where, in polar coordinates, θ is a given etch direction and $R(\theta)$ is the rate for the θ direction. Of course, this $\{R, \theta\}$ vector can also be represented by Cartesian coordinates: $\{x, y\}$. Because of silicon's symmetry, we need only examine 1/8th of the circle: $0 \leq \theta \leq \pi/4$ (or $0 \leq x \leq 1$ and $0 \leq y \leq x$). For example the (10), $(\bar{1}0)$, and (01) vectors have the same rate since they belong to the (10) family. This use of symmetry simplifies the derivation, but the model is in no way limited to symmetrical systems. For asymmetrical systems all regions of the plane must be modeled.

2.1 Two Parameters

In two dimensions, two independent vectors are needed to define a basis. In the two-parameter model there are two distinct rate vectors, the (10) vector at zero degrees and the (11) vector at 45 degrees. These vectors shall be called the principal vectors or principal rates.

These two dimensional rate vectors are the two dimensional projections of the three dimensional etch rates for different planes. The (11) vector is the projection of the (111) plane while the (10) vector is the projection of either the (100) or the (101) plane depending on the etchant being modeled.

In order to interpolate the etch rate of any arbitrary vector we wish to find its components not in terms of its Cartesian components but rather in terms of its (10) and (11) components. In other words we wish to transform from a representation in Cartesian space into a representation in the non-orthogonal basis of the two linearly independent principal rate vectors. We do this by multiplying the $\{x, y\}$ vector by the inverse of the basis matrix defined by the principal vectors. This is equivalent to solving two simultaneous equations to determine what magnitudes of the (10) and (11) vectors are required to construct an arbitrary vector (see Figure 1).

In addition we must satisfy the additional condition that the interpolated rates be isotropic when the (10) and (11) rates are unity. This is done with a diagonal scaling matrix which simply multiplies the result by two scaling constants. In the

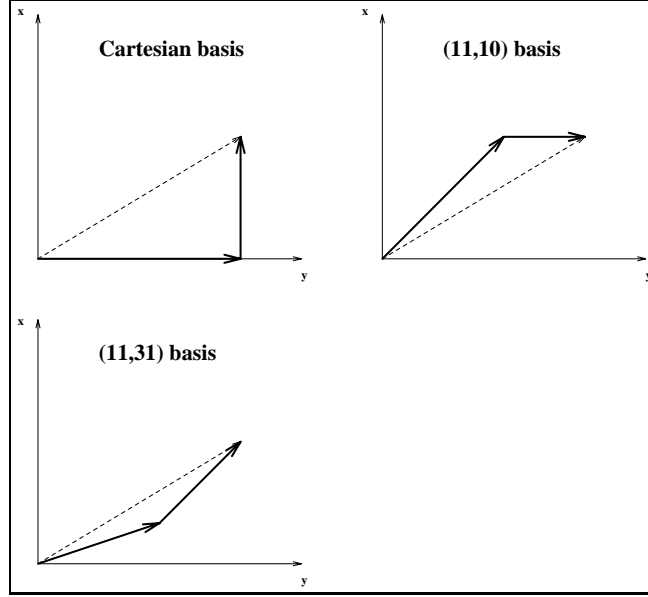


Figure 1: Two dimensional basis representations.

two dimensional two parameter model the scaling matrix is the identity matrix but this is not true in general. If this scaling matrix is not included the model is still valid but the model etch rates will differ from the experimental etch rates. The need for the scaling matrix arises because when the Miller indices are calculated, the numbers are scaled to be integers. The scaling matrix undoes this Miller scaling.

Every vector has a representation in the orthogonal Cartesian basis $\{x, y\}$. Let $\{a, b\}$ be the components of a vector $\{x, y\}$ in the non-orthogonal basis defined by the normals (Miller indices $\{h, k\}$) of two principal planes. Then:

$$\begin{bmatrix} a & b \end{bmatrix} = \begin{bmatrix} x & y \end{bmatrix} \begin{bmatrix} h_1 & k_1 \\ h_2 & k_2 \end{bmatrix}^{-1} \begin{bmatrix} s_1 & 0 \\ 0 & s_2 \end{bmatrix} \quad (1)$$

where s is the scaling matrix. This relationship is valid within the triangular region defined by the two principal planes.

The etch rate along a vector $\{x, y\}$ is then given by a weighted sum of these components. By choosing the weights (W_i) to be the ratio of the i^{th} rate to the (11) rate, it is possible to separate the shape of the etch rate diagram (ratio of rates) from the absolute size of the etch rate diagram ((11) rate). Thus $W_1 = 1$ and $W_2 = R_{(10)}/R_{(11)}$:

$$R(x, y) = N(a * W_1 + b * W_2) * R_{11} \quad (2)$$

where N is a normalization factor ($1/x$ in this case). N is necessary since R should be dependent on angle (ratios of x and y) and not on the magnitudes of x and y . This formula is valid for all possible symmetric etchants: isotropic or highly

<i>basis vectors</i>	<i>scaling matrix</i>	<i>component equations</i>	<i>normalization</i>
$\begin{bmatrix} 1 & 0 \\ 1 & 1 \end{bmatrix}$	$\begin{bmatrix} 1 & 0 \\ 0 & 1 \end{bmatrix}$	$a = x - y$ $b = y$	$1/x$

Table 1: 2D, two parameter model matrices and equations.

anisotropic. Table 1 displays the details of this model. Note that the equations are only valid when a and b are positive, since the weights cannot be negative.

Compared to other planes, the (111) planes are relatively dense. For many etchants they are the slowest etching planes. The ratio of the fastest to slowest planes ranges from 1:1 for the isotropic case to 400:1 for etchants such as KOH. For this reason it is not necessary to plot the etch rate diagrams for the cases where the ratio of (10) to (11) is less than unity, although the model would still be valid if small ratio etchants were available. Figure 2 shows an array of hypothetical ratios of the (10) etch rate to the (11) etch rate. Each element in the array has been scaled to fill an equal amount of space for display purposes. This has been done for all the arrays that follow.

2.1.1 Three Parameters

The effect of the (311) planes can be included by using a three parameter model. Again only the region $0 \leq \theta \leq \pi/4$ is considered, but there are now three principal rates (10), (11), and (31) where the (31) vector is the two dimensional projection of the (311) plane. The (10) and (11) rates appear when etching holes since they are slow compared to faster planes such as the (31) rates. When simulating the etching of pegs, failure to include (31) rates will lead to shapes that are correct in form but incorrect in detail; the three parameter model eliminates this deficiency. The (31) vector lies at about 18 degrees ($\arctan(1/3)$) with respect to the x axis. Because only two vectors at a time may be used as a two dimensional basis, two regions are examined: $0 \leq \theta \leq \arctan(1/3)$ with (10) and (31) as the basis and $\arctan(1/3) \leq \theta \leq \pi/4$ with (31) and (11) as the basis. The derivation for the two parameter model is carried out again for the two regions producing two separate weighted sums each valid within its associated region. In this case the scaling matrix is not the identity matrix but contains a 1 and a 3 along the diagonal. In general, the scaling matrix diagonal value is the maximum Cartesian component of the associated plane. Note that the rates are continuous across the region interface. The net effect of the (31) rates is to produce secondary extrema as shown in Figure 3. The results are rearranged to separate the size and shape effects as was done with Equation 2 in the two parameter model.

Furthermore we can find the value for the (31)/(11) rate ratio required to collapse

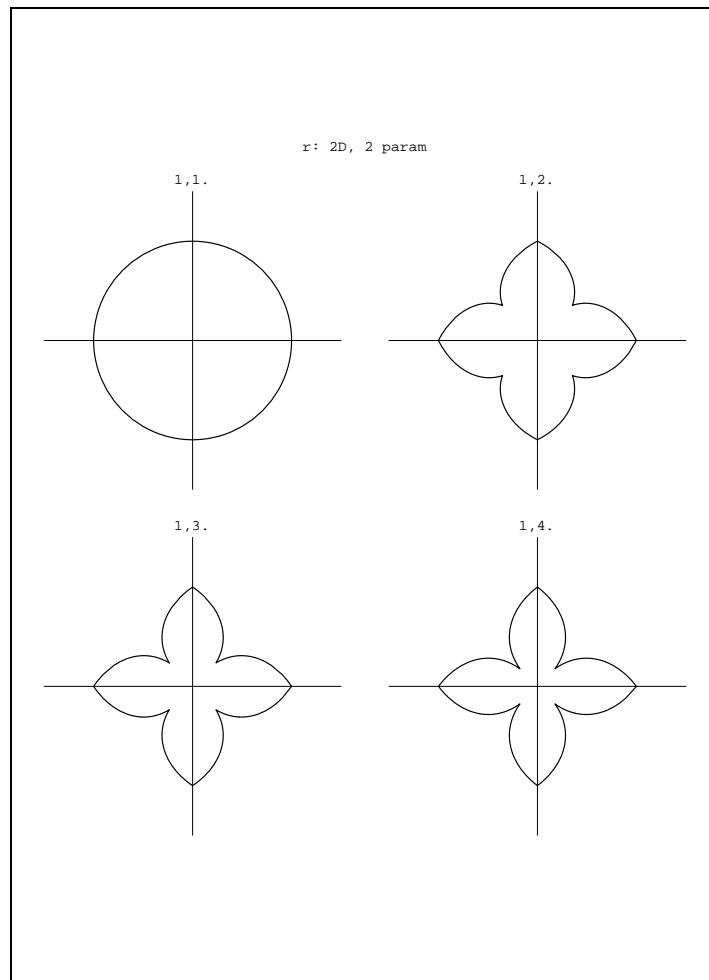


Figure 2: 2D, two parameter results.

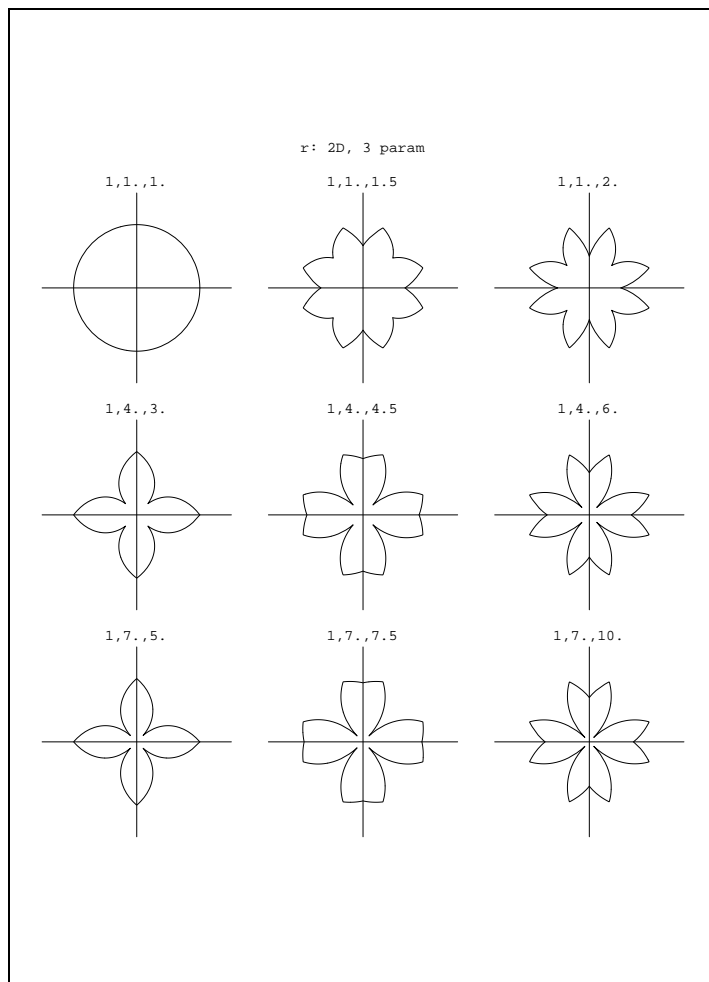


Figure 3: 2D, three parameter results.

the three parameter model to two parameters:

$$(R_{31}/R_{11})_{2p} = (1 + 2 * R_{10}/R_{11})/3$$

Table 2 displays the details of this model. Note that the equations are only valid when a and b are positive, since the weights cannot be negative.

Again the availability of etchants is used to limit the R_{10}/R_{11} rates and the scaling factor to be larger than or equal to unity. Figure 3 shows such plots.

2.2 Three Dimensions

Consider a vector in space defined by its Cartesian components x , y , and z or in spherical coordinates R , θ , and ϕ , where the magnitude of the vector is the three dimensional etch rate in the direction of the vector. Because of silicon's symmetry, we need only look at 1/16th of the sphere: $0 \leq \theta \leq \pi/4$ and $0 \leq \phi \leq \pi/2$ (or

<i>basis vectors</i>	<i>scaling matrix</i>	<i>component equations</i>	<i>normalization</i>
$\begin{bmatrix} 1 & 0 \\ 3 & 1 \end{bmatrix}$	$\begin{bmatrix} 1 & 0 \\ 0 & 3 \end{bmatrix}$	$a = x - 3y$ $b = 3y$	$1/x$
$\begin{bmatrix} 1 & 1 \\ 3 & 1 \end{bmatrix}$	$\begin{bmatrix} 1 & 0 \\ 0 & 3 \end{bmatrix}$	$a = (-x + 3y)/2$ $b = 3/2(x - y)$	$1/x$

Table 2: 2D, three parameter model matrices and equations.

$$0 \leq x \leq 1, 0 \leq y \leq x, 0 \leq z \leq 1 \text{) .}$$

2.2.1 Three Parameters

In three dimensions, three independent vectors are needed to define a basis. The three principal vectors for the three parameter model are the (111), (100), and (110) rates. In this section of the sphere there are 5 principal planes in 3 families:

- (100) family: (100) and (001)
- (110) family: (110) and (101)
- (111) family: (111)

From symmetry, all planes within a family have the same rate. The five planes form three triangular regions on the sphere each bounded by three basis vectors: (100,111,110), (100,111,101), & (001,111,101) as shown in Figure 4.

For each triangular section, the representation of any arbitrary vector is found in the non-orthogonal basis by multiplying the vectors Cartesian components by the inverse of the 3 by 3 basis matrix. Again a scaling matrix is necessary. This is equivalent to solving three simultaneous equations to determine the magnitudes of the (100), (110) and (111) vectors required to construct an arbitrary vector. The required rate is a weighted sum of the components expressed in terms of etch rate ratios.

Every vector has a representation in a orthogonal Cartesian basis $\{x, y, z\}$. Let $\{a, b, c\}$ be the components of a vector $\{x, y, z\}$ in the non-orthogonal basis defined by the normals (Miller indices $\{h, k, l\}$) of three principal planes. Then:

$$\begin{bmatrix} a & b & c \end{bmatrix} = \begin{bmatrix} x & y & z \end{bmatrix} \begin{bmatrix} h_1 & k_1 & l_1 \\ h_2 & k_2 & l_2 \\ h_3 & k_3 & l_3 \end{bmatrix}^{-1} \begin{bmatrix} s_1 & 0 & 0 \\ 0 & s_2 & 0 \\ 0 & 0 & s_3 \end{bmatrix} \quad (3)$$

This relationship is valid within the triangular region defined by the three principal planes. The etch rate at a vector $\{x, y, z\}$ is then given by a weighted sum of

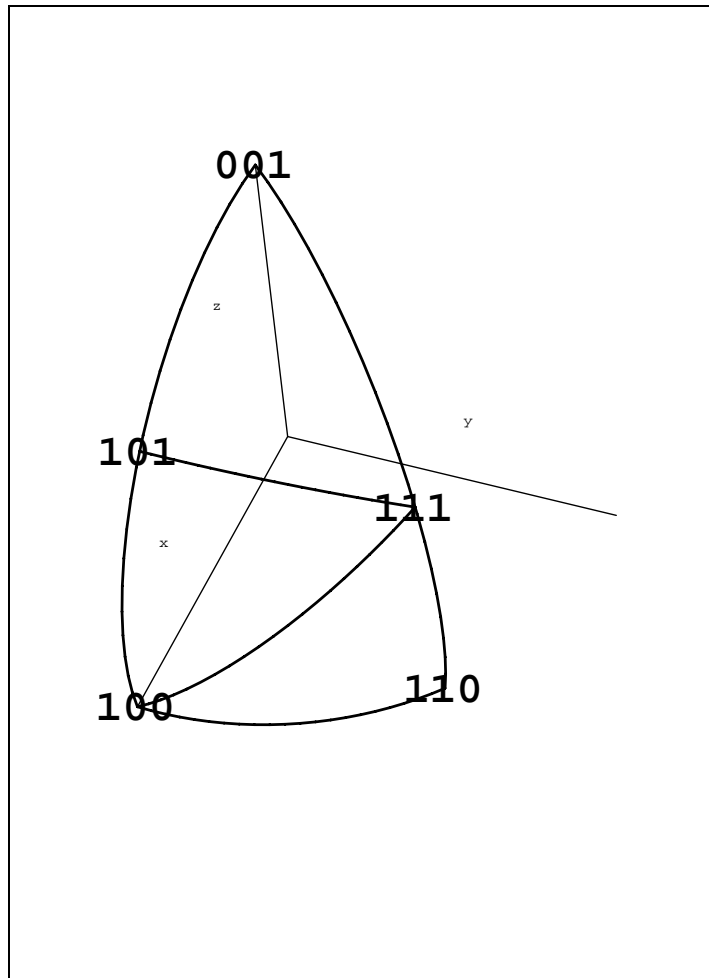


Figure 4: 3D, three parameter model regions.

<i>basis vectors</i>	<i>scaling matrix</i>	<i>component equations</i>	<i>normalization</i>
$\begin{bmatrix} 1 & 0 & 0 \\ 1 & 1 & 0 \\ 1 & 1 & 1 \end{bmatrix}$	$\begin{bmatrix} 1 & 0 & 0 \\ 0 & 1 & 0 \\ 0 & 0 & 1 \end{bmatrix}$	$a = x - y$ $b = y - z$ $c = z$	$1/x$
$\begin{bmatrix} 1 & 0 & 0 \\ 1 & 0 & 1 \\ 1 & 1 & 1 \end{bmatrix}$	$\begin{bmatrix} 1 & 0 & 0 \\ 0 & 1 & 0 \\ 0 & 0 & 1 \end{bmatrix}$	$a = x - z$ $b = z - y$ $c = y$	$1/x$
$\begin{bmatrix} 0 & 0 & 1 \\ 1 & 0 & 1 \\ 1 & 1 & 1 \end{bmatrix}$	$\begin{bmatrix} 1 & 0 & 0 \\ 0 & 1 & 0 \\ 0 & 0 & 1 \end{bmatrix}$	$a = z - x$ $b = x - y$ $c = y$	$1/z$

Table 3: 3D, three parameter model matrices and equations.

these components:

$$R(x, y, z) = N(a * W_1 + b * W_2 + c * W_3) * R_{111} \quad (4)$$

where W_i is the relative etch rate or weight for the i^{th} plane. N is a normalization factor (either $1/x$ or $1/z$) which ensures that the rates are independent of the magnitude of x , y , and z . Two different normalizations are needed to provide continuity on the boundary between regions. Table 3 shows the details of this model. Again a , b , and c must be positive for the equations to be valid.

This formula is valid for all possible symmetric etchants: isotropic or highly anisotropic. Figure 5 shows the etch rates for ratios greater than unity.

2.2.2 Four Parameters

The (311) rates can be added to the model by redefining the triangular sections. In this case there seven vectors in the three principal families:

(100) family: (100) and (001)

(110) family: (110) and (101)

(111) family: (111)

(311) family: (113) and (311)

The new vectors require that the triangular sections be properly chosen. The seven planes form six triangular regions on the sphere each limited by three planes: (100,311,110), (100,101,311), (110,111,311), (101,111,311), (101,113,111), and (001,113,101) as shown in Figure 6.

Figure 5: 3D, three parameter model results.

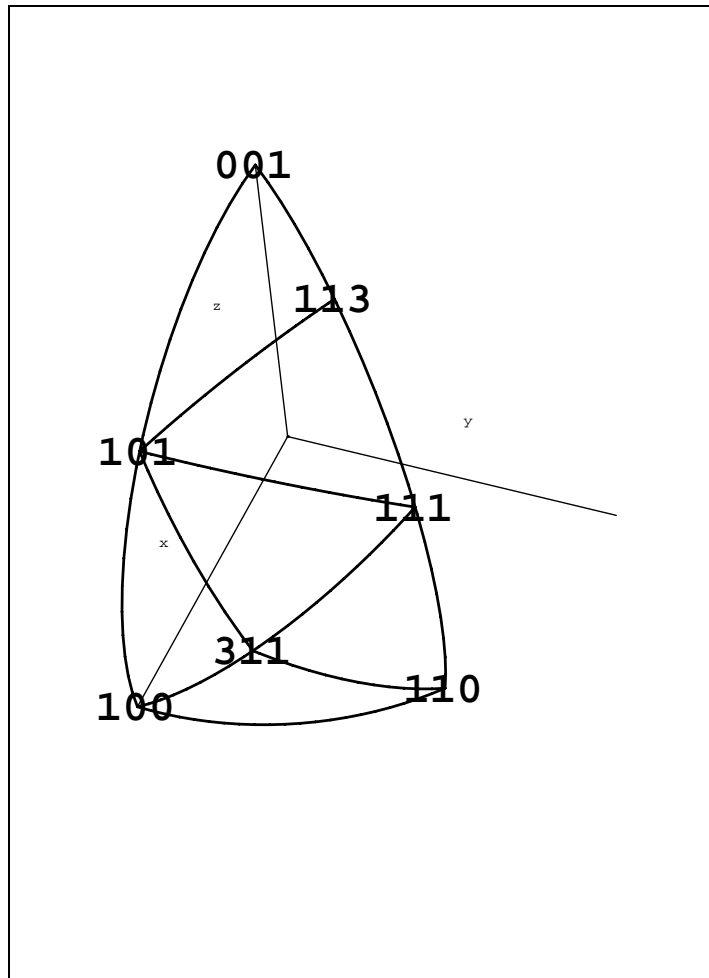


Figure 6: 3D, four parameter model regions.

The etch rate at a vector $\{x, y, z\}$ is then given by a weighted sum of these components. Table 4 shows the details of this model. Figure 7 shows the etch rates for ratios greater than unity.

3 3D \Rightarrow 2D (100) Projections

Given a three dimensional etch rate diagram $R(\phi, \theta)$, some planes will tend to dominate others in certain conditions. One important factor is wafer orientation. The wafer orientation refers to the crystal orientation along which the crystal is cut (the (100) orientation being the most common). This cutting of the wafer establishes boundary conditions which limit the observed etch rates to a subset of the full three dimensional etch rate diagram.

Consider a (100) wafer which is partially masked as shown in Figure 8A. The line separating the masked and unmasked portions lies at some angle θ . A cross section ss (see Figure 8B) is taken perpendicular to the plane of the wafer and perpendicular to θ in order to examine planes with different ϕ values. At each θ , the two dimensional etch rate along the surface of the wafer can now be found. Figure 8B shows the cross section ss with two representative rates R_1 and R_2 . The observed surface etch rate is given by the minimum projection onto the surface of the wafer. For a (100) wafer the minimum surface projection is:

$$R_{2d}(\theta) = \min_{\phi}[proj(\theta, \phi)] \Rightarrow proj(\theta, \phi) = R_{3d}(\theta, \phi) / \cos(\phi - 90) \quad (5)$$

Thus the observed surface etch rate at θ depends on all the rates and ϕ 's in the cross section perpendicular to the wafer. In practice, this minimization is performed over many ϕ values although only two are shown in Figure 8B for clarity.

In addition to the surface etch rate, much more information may be obtained using additional projections. The plane of the wafer corresponds to a ϕ value of 90 degrees. It is possible to extend this minimization to other projections made onto different cross sections at different angles with respect to the wafer. Note that the cross sections are still at the same θ . Let α be the ϕ value of the different cross sections. Figure 9 again shows rates R_1 and R_2 with projections onto three cross sections at three α 's : 90 (plane of wafer), 60, and 30 degrees (s90, s60, and s30 respectively). In the figure the projections of R_2 with s30, s60, and s90 are given by $p(30)_2$, $p(60)_2$, and $p(90)_2$ respectively.

The $\alpha=90$ corresponds to the surface etch rate while the $\alpha=60$ and $\alpha=30$ give information about the etch rate deeper into the crystal. Thus there are three contours to plot the etch rate behavior. Adding more contours provides more information about the observed etch rates. Closely packed contours indicate sharply sloped walls while widely spaced contours indicate walls with smaller slopes. Note that each contour represents constant α and not constant depth. Figure 10 shows a modeled (100) projection while Figure 11 shows experimental data.

It is important to note that the transformation from three dimensions to two is a projection. The two dimensional etch rate diagram is not a shadow of the three dimensional diagram nor is it a slice through the three dimensional diagram.

<i>basis vectors</i>	<i>scaling matrix</i>	<i>component equations</i>	<i>normalization</i>
$\begin{bmatrix} 1 & 0 & 0 \\ 1 & 1 & 0 \\ 3 & 1 & 1 \end{bmatrix}$	$\begin{bmatrix} 1 & 0 & 0 \\ 0 & 1 & 0 \\ 0 & 0 & 3 \end{bmatrix}$	$a = x - y - 2z$ $b = y - z$ $c = 3z$	$1/x$
$\begin{bmatrix} 1 & 0 & 0 \\ 1 & 0 & 1 \\ 3 & 1 & 1 \end{bmatrix}$	$\begin{bmatrix} 1 & 0 & 0 \\ 0 & 1 & 0 \\ 0 & 0 & 3 \end{bmatrix}$	$a = x - 2y - z$ $b = z - y$ $c = 3y$	$1/x$
$\begin{bmatrix} 1 & 1 & 1 \\ 1 & 1 & 0 \\ 3 & 1 & 1 \end{bmatrix}$	$\begin{bmatrix} 1 & 0 & 0 \\ 0 & 1 & 0 \\ 0 & 0 & 3 \end{bmatrix}$	$a = (y - x)/2 + z$ $b = y - z$ $c = 3/2(x - y)$	$1/x$
$\begin{bmatrix} 1 & 1 & 1 \\ 1 & 0 & 1 \\ 3 & 1 & 1 \end{bmatrix}$	$\begin{bmatrix} 1 & 0 & 0 \\ 0 & 1 & 0 \\ 0 & 0 & 3 \end{bmatrix}$	$a = (2y - x + z)/2$ $b = z - y$ $c = 3/2(x - z)$	$1/x$
$\begin{bmatrix} 1 & 1 & 1 \\ 1 & 0 & 1 \\ 1 & 1 & 3 \end{bmatrix}$	$\begin{bmatrix} 1 & 0 & 0 \\ 0 & 1 & 0 \\ 0 & 0 & 3 \end{bmatrix}$	$a = (x + 2y - z)/2$ $b = x - y$ $c = 3/2(z - x)$	$1/z$
$\begin{bmatrix} 0 & 0 & 1 \\ 1 & 0 & 1 \\ 1 & 1 & 3 \end{bmatrix}$	$\begin{bmatrix} 1 & 0 & 0 \\ 0 & 1 & 0 \\ 0 & 0 & 3 \end{bmatrix}$	$a = -x - 2y + z$ $b = x - y$ $c = 3y$	$1/z$

Table 4: 3D, four parameter model matrices and equations.

Figure 7: 3D, four parameter model results.

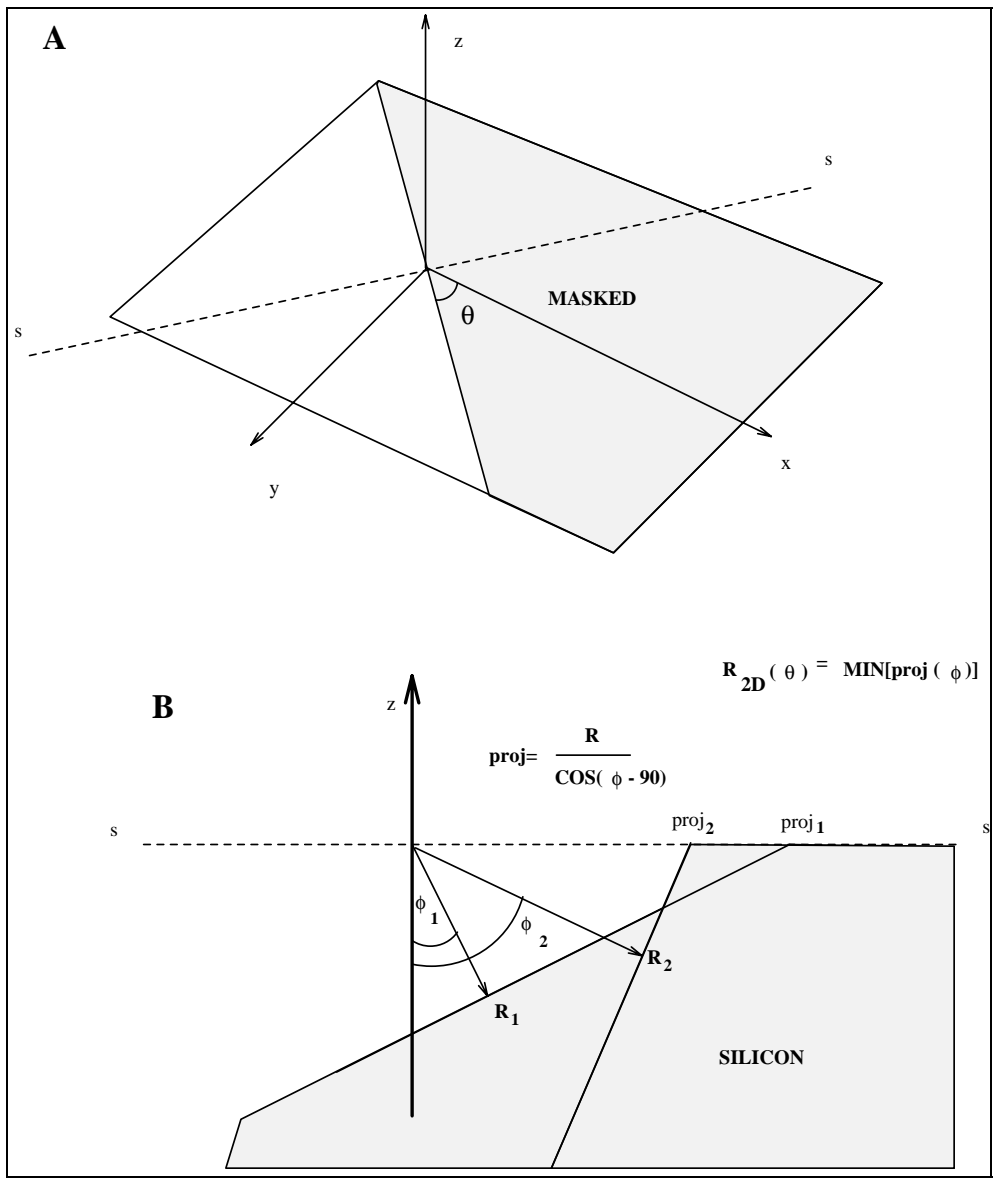


Figure 8: Minimum projection.

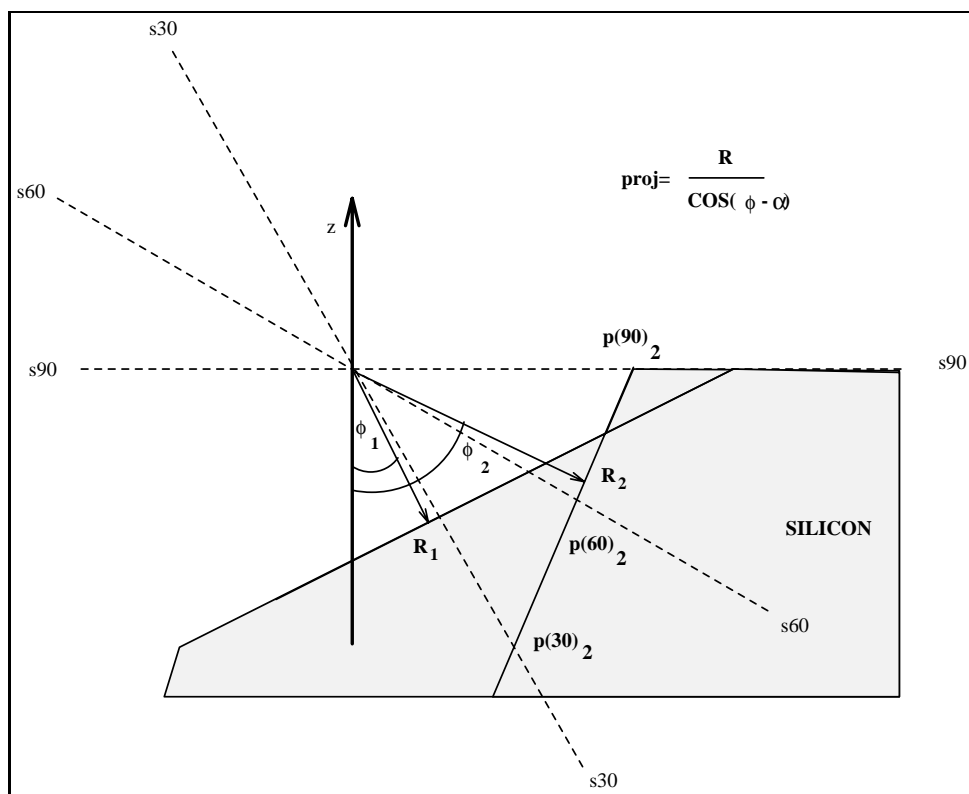


Figure 9: Projections onto different cross sections.

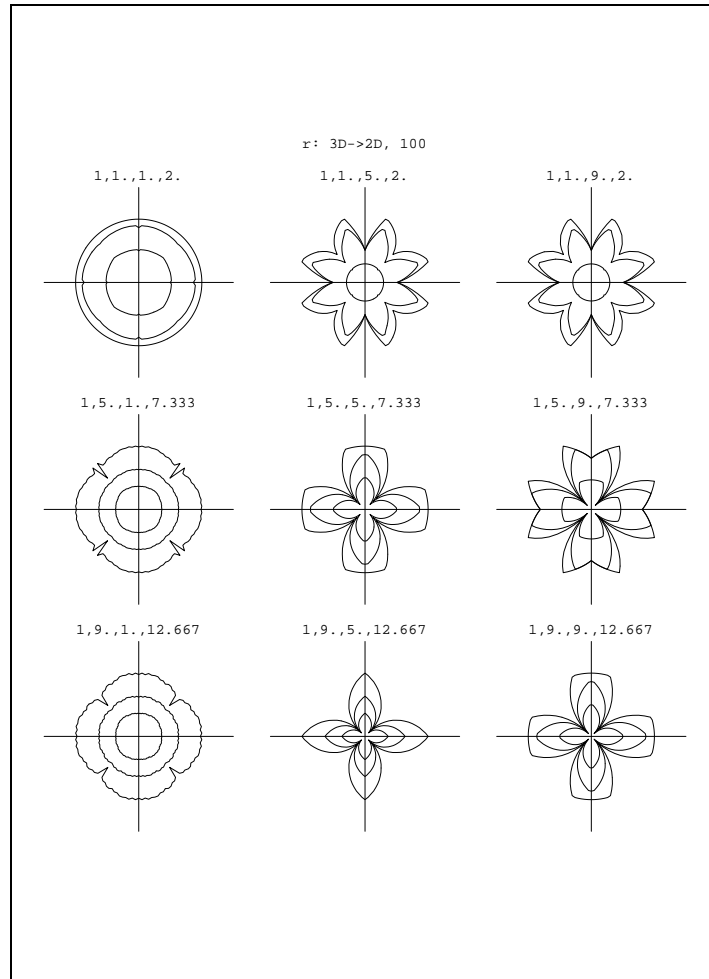


Figure 10: Modeled (100) projection. Outer contours show etch rate at surface, inner contours show etch rate at greater depths.

Figure 11: Experimental (100) projection.

3.1 General Projections

Projections need not be limited to the (100) plane.

Consider a new wafer cut (abc) rotated from the (100) frame by $\Delta\phi$ and $\Delta\theta$. Coordinates in the (100) frame are given by (ϕ, θ) , coordinates in the (abc) frame are given by (ϕ_2, θ_2) .

If the orientation of the wafer cut is changed, the projection planes also change. There are two approaches to finding the new projections. One possible approach is to explicitly calculate these new projections. Alternatively, the reference frame of the rate diagram can be rotated to the new orientation and the (100) projection is used as before. This second approach will be used since it is simpler.

Let $R_{100}(\theta, \phi)$ be the rate defined in the (100) frame. Each such rate corresponds to a rate in the rotated (abc) frame: $R_{abc}(\theta_2, \phi_2)$. In the case of a (100) wafer, at each θ , a minimization over ϕ is performed using $R_{100}(\theta, \phi)$. Projections onto another plane (abc) are found by replacing $R_{100}(\theta, \phi)$ with $R_{abc}(\theta_2, \phi_2)$ before performing the minimization.

The spherical coordinates in the new (abc) reference frame defined by the new wafer cut must be converted into the spherical coordinates in the (100) reference frame. The equations giving the new coordinates are :

$$\cos(\phi_2) = \cos(\Delta\phi) \cos(\phi) - \cos(\theta) \sin(\Delta\phi) \sin(\phi) \quad (6)$$

$$\begin{aligned} \cos(\theta_2) \sin(\phi_2) &= \cos(\Delta\theta) \cos(\phi) \sin(\Delta\phi) \\ &+ \cos(\Delta\phi) \cos(\Delta\theta) \cos(\theta) \sin(\phi) \\ &- \sin(\Delta\theta) \sin(\phi) \sin(\theta) \end{aligned} \quad (7)$$

For the (110) wafer $\Delta\theta = \pi/4$ and $\Delta\phi = 0$, while for the (111) wafer $\Delta\theta = \pi/4$ and $\Delta\phi = \pi/4$. The minimization is performed as before but the rate values used are those obtained from the new angles. Figure 12 shows such a (110) projection. Figure 13 shows experimental measurements of the (110) projection (reproduced from a paper by Seidel [12]).

4 Generality

In this derivation the (111), (110), (100), and (311) rates have been chosen as principal planes. These planes were chosen because they appear quite often in the anisotropic etching of silicon. The model is in no way limited to such systems and any three principal planes may serve as a basis. More planes may be added to increase the accuracy of the model, in which case new triangular regions will have to be defined.

5 Summary

A method for parametrizing the full three dimensional etch rate behavior given a few known rates has been presented and found to agree with experimental measurements.

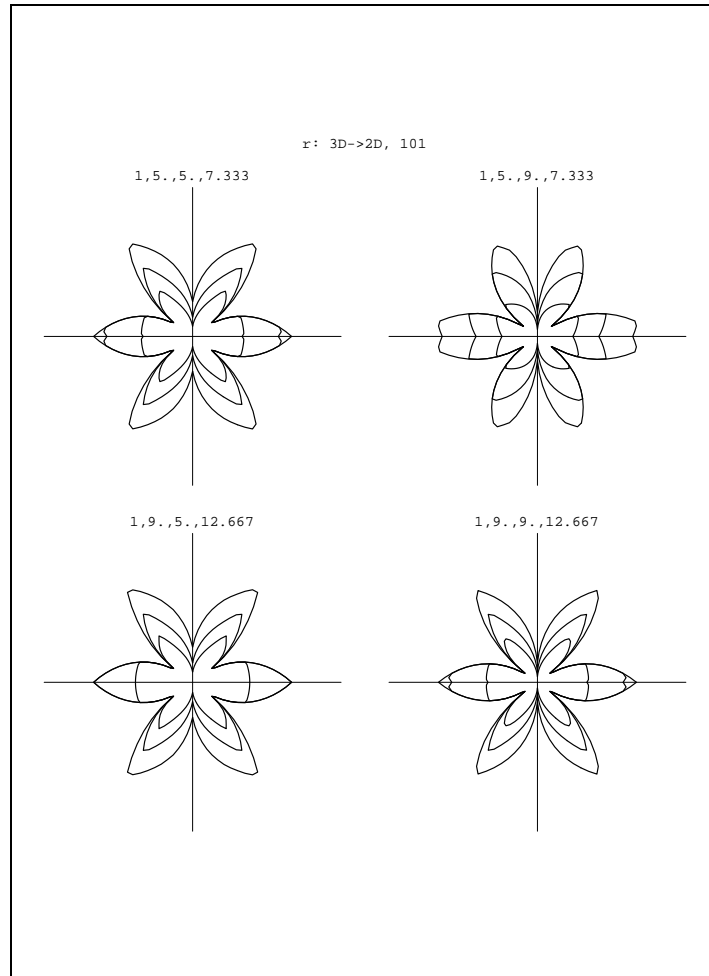


Figure 12: Modeled (110) projection. Outer contours show etch rate at surface, inner contours show etch rate at greater depths.

Figure 13: Experimental (110) projection from Seidel et al. [12].

The model does not seek to understand the reasons why etch rates differ, but rather uses the known available data to predict the results of differing etch rates. The method clarifies both the three dimensional nature of the etch rate diagram as well as the observed etch rates for different wafer planes. The predictions of any MEMS CAD tools can only be as good as the data it is provided. A standardized system for measuring and classifying different etchant based on their etch rate behavior is a much needed aspect of MEMS design. The model outlined above is a valuable part of such a system.

Acknowledgments

The authors wish to gratefully acknowledge Professor Y.C. Tai for the use of his facilities and many helpful discussions. This material is based upon work supported, in part, by the National Science Foundation under Grant No. ECS-9023646. Any opinions, findings, conclusions or recommendations expressed in this publication are those of the authors and do not necessarily reflect the views of the sponsor.

References

- [1] G. DeLapierre. Anisotropic crystal etching: A simulation program. *Sensors and Actuators*, 31:267–274, 1992.
- [2] S. D. Senturia, R. M. Harris, B. P. Johnson, S. Kim, M. A. Shulman, and J. K. White. A computer-aided design system for microelectromechanical systems (MEMCAD). *Journal of Microelectromechanical Systems*, 1:3–13, March 1992.
- [3] D. W. Shaw. Morphology analysis in localized crystal growth and dissolution. *J. Cryst. Gr.*, 47:509–517, 1979.
- [4] T. Thurgate. Segment based etch algorithm and modeling. *IEEE Transactions on computer-aided design*, pages 1101–1109, sep 1991.
- [5] Ted J. Hubbard and Erik K. Antonsson. Emergent Faces in Crystal Etching. *Journal of Microelectromechanical Systems*, 3(1):19–28, March 1994.
- [6] Ted J. Hubbard and Erik K. Antonsson. Cellular Automata in MEMS Design. *Journal of Microelectromechanical Systems*, 1994. Submitted for review, July, 1994, EDRL-TR 94d.
- [7] C. H. Sequin. Computer simulation of anisotropic crystal etching. In *Transducers '91*, pages 801–806, San Francisco, CA, USA, 1991.
- [8] R. A. Buser and N. F. de Rooij. ASEP: A CAD program for silicon anisotropic etching. *Sensors and Actuators*, 28:71–78, 1991.
- [9] E. Herr and H. Balles. KOH etching of high index crystal planes in silicon. *Sensors and Actuators*, 31:283–287, 1992.

- [10] A. Koide, K. Sato, and S. Tanaka. Simulation of two dimensional etch profile of silicon during orientation-dependent anisotropic etching. In *Transducers '91*, pages 216–220, Institute of Electrical Engineers, 1991.
- [11] U. Schnakenberg, W. Benecke, and B. Lochel. NH₄ OH - based etchants for silicon micromachining. *Sensors and Actuators*, A21-A23:1031–1035, 1990.
- [12] H. Seidel, L. Csepregi, A. Heuberger, and H. Baumgartel. Anisotropic etching of crystalline silicon in alkaline solutions. *J. Electrochem. Soc.*, 137:3613–3631, 1990.
- [13] D. F. Weirauch. Correlation of the anisotropic etching of single crystal silicon spheres and wafers. *J. Appl. Phys.*, 46:1478–1483, 1975.